Causal Discovery on HBSC Data

Daryna Nedilko gtb950

June 25, 2025

Abstract

In this study, we explore the causes of bullying and cyberbullying in the digital age, focusing on adolescents in Ukraine. Using constraint-based causal discovery methods, specifically the Fast Causal Inference (FCI) algorithm, we analyse data from the 2018 Health Behaviour in School-aged Children (HBSC) self-report questionnaire. These methods rely on conditional independence tests for discrete data to recover Partial Ancestral Graphs (PAGs) and uncover both the presence and direction of causal pathways. Our findings highlight *beenbullied* as a central node in the causal structure, influenced by traditional and cyber forms of bullying, and linked to school pressure, peer acceptance, and family communication. Contrary to previous notions that digital technology alone drives bullying behaviours. Instead, our results suggest that bullying is deeply rooted in broader social dynamics, signalling that effective prevention must shift its focus to influence school climate, peer relationships, and family support structures.

Contents

1 Introduction

Bullying and its variations are serious problems that are on the rise among adolescents and children [7] and are recognised as a significant public health issue. They are said to impact young individuals, affecting their mental health and prompting harmful or risky behaviours. Bullying has existed for generations, while cyberbullying is a more recent phenomenon arising from the widespread use of digital devices. Some argue, perhaps too readily, that an individual's digital presence incites malicious behaviour. These notions stem primarily from apprehension towards the largely unregulated virtual space. Current moderation of websites and apps is inadequate to safeguard against or prevent violent outbursts.

However, is it wise to view the digital world as the root of the problem concerning increasing aggression levels in children? The issue should be considered in a broader context, examining how environmental factors influence the development of bullying tendencies. In this report, we assume that the internal motivation for cyberbullying and bullying is not significantly different. We propose that cyberbullying has a lower threshold for entry, driven by factors such as anonymity, accessibility, and the absence of direct social feedback in digital spaces. These elements make it easier for individuals, particularly adolescents, to engage in bullying behaviours online than in traditional, face-to-face settings.

To further explore additional factors shaping the mindset of bullies, we will apply causal discovery methods to data from the 2018 Health Behaviour in School-aged Children(HBSC) self-report questionnaire. We will focus our analysis on data from Ukraine.

Causal Discovery aims to uncover causal relationships among multiple variables in a data-driven manner. This approach seeks to understand causality within an entire system of variables, which causal graphs can effectively visualise. A graph $\mathcal{G} = (V, \mathcal{E})$, where V is the set of vertices or nodes and $\mathcal{E}$ is the set of edges that connect these nodes and form the skeleton of the graph. Nodes correspond to the variables in the dataset, while edges represent connections between these variables. Edges can be directed, undirected, bidirected, or have no edge between two nodes.

A graph containing only one-way directed edges and no cycles is called a Directed Acyclic Graph (DAG). In a DAG, an edge direction represents a belief that there is a direct causal relation between two variables. For example, an edge $X \to Y$ means that variable X causes Y. An absence of an edge represents that there is no direct relation, and the variables are marginally independent, hence d-separated on the graph given the set $\mathbf{S} = \{\emptyset\}$, according to the causal Markov property.

D-separation is a graphical criterion used to determine whether a set of variables is conditionally independent of another set, given a third set ($X \perp_G Y \mid \mathbf{S}$). We can infer d-separation statements from data, relying on the faithfulness assumption.

$$X \perp\!\!\!\perp_P Y \mid \mathbf{S} \implies X \perp_G Y \mid \mathbf{S},$$

And use the global Markov property to generate the learned distribution.

$$X \perp_G Y \mid S \implies X \perp\!\!\!\perp_P Y \mid S,$$

Together, these properties establish a correspondence between the conditional independencies observed in the data and the d-separation statements in the graph.

Every DAG encodes a set of d-separation statements, and a DAG can be learned from such statements. However, it is not always possible to learn a unique DAG from the data. Instead, one can identify a Markov Equivalence Class (MEC) of DAGs that share the same skeleton and v-structures, which is represented by a Completed Partially Directed Acyclic Graph (CPDAG). CPDAGs contain both directed and undirected edges. The presence of an undirected edge in a CPDAG indicates a connection between two variables, but the causal direction cannot be determined due to insufficient information in the data.

A graph that contains all kinds of edges (directed, undirected, and bidirected) is called a mixed graph. A bidirected edge between nodes, e.g., $X \leftrightarrow Y$, indicates the presence of a common unobserved (latent) confounder Z such that $X \leftarrow Z \to Y$. A mixed graph is called ancestral if it contains no directed cycles or almost (partially) directed cycles, and for any undirected edge $X - Y$, the nodes X and Y have no parents or spouses. A Directed Acyclic Graph (DAG) is a special case of an ancestral graph containing only directed edges and no cycles. The graph is called maximal if for any two non-adjacent nodes, there exists a set of vertices that m-separates them. M-separation is a generalisation of d-separation for more complex graphs such as Maximal Ancestral Graphs (MAGs).

Similar to DAGs, it might be difficult to learn a MAG from data. However, we can extract a Markov Equivalence Class (MEC) of MAGs by learning a Partial Ancestral Graph (PAG). Markov equivalence rules for MAGs are more complex as for DAGs: a set of MAGs form a MEC if and only if, besides having the same skeleton and unshielded colliders, they also satisfy the condition if a path p is a discriminating path for a vertex V in both graphs, then V is a collider on p in one graph if and only if it is a collider on p in the other. This additional rule ensures that discriminating paths are consistent across equivalent MAGs, maintaining the equivalence beyond what skeletons and unshielded colliders can capture. PAGs represent these equivalence classes. They encode all possible causal structures consistent with the observed data and latent confounding.

Various algorithms can be employed to uncover these relationships from observational data. m-separations are learned from data using conditional independence testing. In this particular report, we will focus on constraint-based methods that utilise conditional independence tests for discrete data to understand both the presence and direction of a causal path in the chosen dataset. We aim to to apply the FCI algorithm and retrieve a PAG that describes causal relations between the environment and bullying in teenagers aged 11 to 16 years, based on HBSC data, and to interpret and analyze the results of a selected algorithm while considering possible improvements, advantages, and drawbacks of the chosen approach.

2 Data Description and Preparation

We use the 2018 Health Behaviour in School-aged Children (HBSC) dataset, a cross-national survey supported by the WHO, which gathers health-related information from adolescents aged 11, 13, and 15. This dataset encompasses over 120 variables and covers areas such as well-being, social relationships, behaviours, and demographic characteristics across more than 40 countries. Detailed description of each variable available in the official report [3].

These variables offer in-depth insights into individuals' health, well-being, and lifestyles. Furthermore, they include indicators related to family structure, affluence, and socio-economic status. For our research, the most critical variables are those measuring the frequency of bullying and how well individuals perceive their social integration within groups, including school peers and friends, the expression of their emotions, and their overall life satisfaction(See Table 2 - key categories are in bold).

The dataset includes two computed indicators:

- `IRFAS` – Family Affluence Scale III (continuous score)
- `IRRELFAS` – Relative family affluence category (categorical: low, medium, high)

IRRELFAS_LMH	**IRFAS**
1 - Lowest 20pct	1, 2, 0, 5, 6, 3, 4, 7, 8, 9
2 - Medium 60pct	6, 4, 5, 8, 9, 3, 7, 11, 10, 12, 2, 1
3 - Highest 20pct	11, 10, 12, 13, 9, 7, 8, 6

Table 1: Relative Family Affluence Score (categorical) and corresponding unique FAS III scores

Variables such as IRFAS and IRRELFAS_LMH are determined by a set of indicators that reflect family affluence. Despite a noticeable gap of nearly 6 points in the average weighted FAS III score for Luxembourg and Armenia (Figure 1), the weighted mode of Relative FAS remains consistent across all regions at a medium level. This prompted us to investigate the relationship between the continuous and categorical versions of the score. McCormack (2011) states that FAS is calculated using the following scheme: Responses to individual items are summed to derive a total FAS score, which is then categorised into three groups: low FAS score (0 to 4), medium FAS score (5 or 6), or high FAS score (7 or 8). However, as one can observe in the table 1, it does not accurately reflect the real data setup, as countries with different FAS III have very similar Relative FAS III distributions A. Therefore, we chose to disregard the categorical version of the score and treated the continuous score as a categorical value, as it is an integer that varies from 0 to 13. The value is set to None if a respondent has not answered any of the component questions. Other than that, we deem FAS III redundant for our further analysis, as it is a resulting variable for other socio-economic backgrounds of an individual[Table 2].

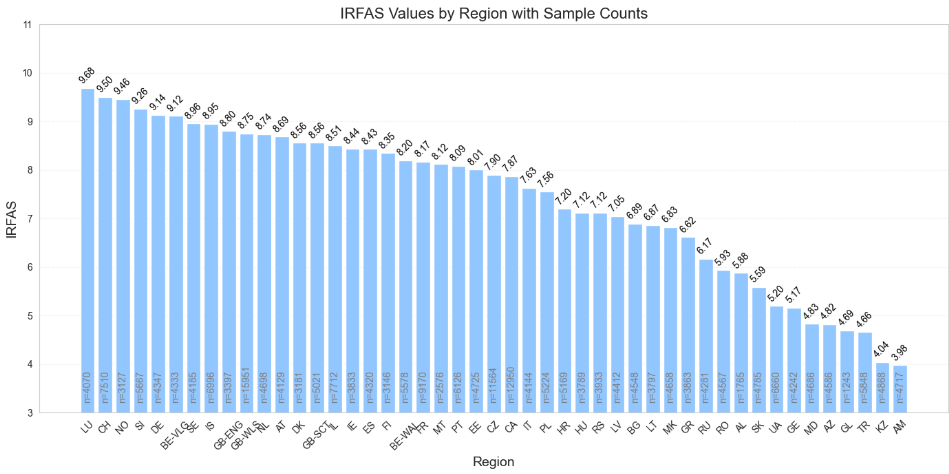

Figure 1: Average IRFAS score by region. The black number indicates the IRFAS score, while the grey number (n=) represents the sample size for each region.

As part of this report, we have decided to focus on data from Ukraine, denoted as region UA in the dataset, or country number 804000. Data acquisition in Ukraine was performed in April and May 2018 using pen-and-paper surveys. Since we are focusing on only one country, it makes sense to ignore columns that have a single value throughout, such as `HBSC`, `cluster`, `countryno`, `adm`, `month`, and `year`. Alongside these, we will exclude any metadata like IDs or data weights from the causal analysis.

Moreover, most of the variables are categorical or discrete. All continuous variables have categorical counterparts, so we will use those instead. Generally speaking, demographics [Table 2] and the rest of the variables can be important and serve as confounders or mediators. Therefore, we decided to examine each category closely and select variables that contribute most to analyzing the reasons and causes of bullying in children. We keep in mind that we are interested in variables that influence bullying.

Table 2 reflects a larger subset of variables considered for the analysis. However, we also focus on a subset of 27 variables: `bulliedothers`, `beenbullied`, `cbulliedothers`, `cbeenbullied`, `fight12m`, `lifesat`, `famhelp`, `famsup`, `famtalk`, `famdec`, `friendhelp`, `friendcounton`, `friendshare`, `friendtalk`, `likeschool`, `schoolpressure`, `studtogether`, `studhelpful`, `studaccept`, `teacheraccept`, `teachercare`, `teachertrust`, `timeexe`, `talkfather`, `talkstepfa`, `talkmother`, and `talkstepmo`. We deem these variables to provide the most information on the subject of bullying and cyberbullying.

We exclude deterministic variables such as `IRFAS`, `IRRELFAS_LMH`, `MBMI`, `IOTF4`, and `oweight_who` from our analysis, alongside variables irrelevant to bullying, such as those related to sexual health and health behaviours like smoking, drinking, and food consumption (see Table 2).

2.1 Data Issues and Preprocessing

- Missing data is handled for us so that we won't get stuck on it for too long. In the original report [3], randomly missing values coded as sysmiss and represented as 'Nones' in the dataset are shown. Besides that, there are also more types of

Category	Include Variables	Exclude Variables
Demographics & Metadata	agecat, sex	HBSC, seqno_int, cluster, id1, id2, id3, id4, weight, adm, month, year, countryno, monthbirth, yearbirth, grade, region, age
Family Affluence Scale	fasfamcar, fasbedroom, fascomputers, fasbathroom, fasdishwash, fasholidays	IRFAS, IRRELFAS_LMH
Health & Wellbeing	health, lifesat, thinkbody, headache, stomachache, backache, feellow, irritable, nervous, sleepdificulty, dizzy	MBMI, IOTF4, oweight_who
Health Behaviors	physact60, timeexe	breakfastwd, breakfastwe, fruits_2, vegetables_2, sweets_2, softdrinks_2, fmeal, toothbr, smokltm, smok30d_2, alcltm, alc30d_2, drunkltm, drunk30d, cannabisltm_2, cannabis30d_2
Body Measures	bodyweight, bodyheight	-
School Experience	likeschool, schoolpressure, studtogether, studhelpful, studaccept, teacheraccept, teachercare, teachertrust	-
Violence and Bullying	bulliedothers, cbulliedothers, fight12m, injured12m, beenbullied, cbeenbullied	-
Peer Support	friendhelp, friendcounton, friendshare, friendtalk	-
Emotional Communication	emconlfreq1-4, emconlpref1-3, emcsocmed1-9	-
Sexual Health	-	hadsex, agesex, contraceptcondom, contraceptpill
Migration Background	countryborn, countrybornmo, countrybornfa	-
Household Composition	motherhome1, fatherhome1, stepmohome1, stepfahome1, fosterhome1, elsehome1_2	-
Parental Employment	employfa, employmo, employnotfa, employnotmo	-
Parent-Child Communication	talkfather, talkstepfa, talkmother, talkstepmo	-
Family Support	famhelp, famsup, famtalk, famdec	-

Table 2: 120 fields from the HBSC dataset categorized according to the content of their corresponding survey questions. Inclusion selection was guided by theoretical importance, relevance as confounders or mediators, and direct links to bullying outcomes. Certain variables were excluded because they are derived from, or fully determined by, other variables already included in the dataset.

missingness observed in data, such as "Missing due to skip pattern"(99) or "Missing due to inconsistent answer"(-99). Fortunately, 99 and -99 missingness types are not present in our subset of data. Since the rest is missing completely at random, by assumption, we drop the records with missing values, accounting for the qualities of FCI to handle selection bias[6] that might occur after such data manipulation.

- For the few continuous ones, we selected their discrete counterparts where available. All categorical string variables were label-encoded into integers.
- The resulting sample size for Ukraine is 6,660 records. This is sufficient to produce statistically meaningful results, even after removing records with missing values.
- We acknowledge that using only Ukrainian data limits generalizability.

3 Methodology

For this report, we focus on constraint-based algorithms, namely Fast Causal Inference (FCI). The constraint-based approach to causal discovery employs conditional independence(CI) testing or m-separation constraints to recover features of the causal MAG. For the results to be valid, a set of assumptions must hold to ensure that statistical independence reflects the actual absence of causation. FCI is a global search algorithm, meaning it uncovers the full relationship graph between variables in the dataset.

3.1 Assumptions

- **A1. Causal Markov Condition**
  For any variable X, given its direct causes PA_X, X is conditionally independent of its non-descendants:
  $$X \perp\!\!\!\perp_G \mathrm{ND}_X \mid \mathrm{PA}_X$$
- **A2. Relaxed Causal Sufficiency**
  Not all common causes (confounders) are observed. Latent variables L may induce dependencies such that:
  $$X \not\perp\!\!\!\perp Y \mid Z \quad \text{even if} \quad X \perp\!\!\!\perp Y \mid Z, L$$
- **A3. Faithfulness**
  All and only the conditional independencies observed in the data correspond to d-separations in the true causal graph:
  $$X \perp\!\!\!\perp Y \mid Z \Rightarrow X \text{ and } Y \text{ are d-separated by } Z \text{ in the graph}$$
- **A4. CI Tests Suitability and Correctness**
  The CI tests or the oracle used must reliably detect:
  $$X \perp\!\!\!\perp Y \mid Z$$
  with high statistical power and controlled Type I error based on the sample data.

3.2 Fast Causal Inference

The algorithm consists primarily of two stages. In the first stage, it identifies the adjacencies in the causal MAG. The inference of these adjacencies is based on the principle that two variables are adjacent in a MAG if and only if they are not m-separated by any set of other variables in the graph. Essentially, the algorithm searches for every pair of variables to find a set of other variables that makes them conditionally independent. They are not considered adjacent if such a set is found. If all assumptions are fulfilled, the FCI algorithm successfully determines the correct adjacencies.

The second stage involves inferring edge marks. During this stage, the algorithm applies a series of orientation rules (as referenced in [6]) to introduce arrowheads or tails, with circles ($\circ$) representing undetermined edge marks. The final output of the algorithm is PAG, which means the Markov equivalence class as determined by the oracle of CI.

3.3 CI tests

Having clear m-separation statements would require an oracle capable of providing the correct CI information. In practice, CI tests are used to approximate m-separation statements, which describe a MAG. These tests determine weather X and Y are conditionally independent given a conditioning set $S = \{s_1, \dots, s_d\}$, where d is the number of nodes in the set. In other words, the test checks whether S serves as a separating set (Sepset) for X and Y in the learned graph. If $S = \emptyset$, the test is for marginal independence between X and Y.

CI tests operate using a significance level α, which is an arbitrary threshold determining whether the observed (in)dependence is statistically significant. CI tests are also used for marginal independence when $S = \emptyset$. However, they only reflect the conditional independencies present in the observed data, which may not perfectly align with those in the true underlying causal structure. These tests are prone to errors, particularly with small sample sizes. Mistakes made early in the discovery process, such as incorrectly removing an edge due to a false detection of independence, can result in incorrect graph structures later(error propagation).

Statistical CI Tests for Discrete Data

The most commonly used CI tests for discrete data are the G^2 and χ^2 statistical tests. Both assume a null hypothesis stating that variables A and Y are conditionally independent given a set of variables S. These tests yield a statistic in the form of a p-value, indicating the probability of observing the data under the null hypothesis. If the p-value falls below the chosen significance level α, the null hypothesis is rejected, suggesting that A and Y are conditionally dependent.

The general form of the G^2 Test statistic(likelihood-ratio test statistic) is as follows:

$$G^2 = 2 \cdot \sum \text{Observed} \cdot \ln\left(\frac{\text{Observed}}{\text{Expected}}\right)$$

When conditioning on S, the observed and expected values are defined as:

$$\text{Observed} = N_{\text{obs}} \quad \text{and} \quad \text{Expected} = \frac{N_{\text{ys}} \cdot N_{\text{xs}}}{N_s}$$

Thus, the G^2 statistic can be expressed as:

$$G^2 = 2 \cdot \sum_{x,y,s} N_{\text{xys}} \ln \left(\frac{N_{\text{xys}} N_s}{N_{\text{xs}} N_{\text{ys}}} \right)$$

Here, x and y range over the values of variables X and Y, while s covers all combinations of values within the set S. In this context, N represents the size of the corresponding subset. The p-value is calculated under the assumption that none of the values N_{xys} is zero, meaning that every possible combination of values is present in the data. If any combination has N_{xys} equal to zero, we heuristically reduce the degrees of freedom (df) for the p-value for each such combination. It is calculated under the assumption that none of the values N_{xys} is zero[4].

χ^2 **Test** is similar to G^2, but define as:

$$\chi^2 = 2 \cdot \sum \frac{(Observed - Expected)^2}{Expected}$$

The tests are asymptotically equivalent and converge similarly for small datasets.

3.4 Algorithm Description

3.4.1 Input

The algorithm takes as input three components: a dataset, a CI test and a significance level α for the CI tests. The dataset should include the variables of interest. The data can be continuous, discrete, or mixed. Significance level(α): Typically 0.05, to determine whether to reject the null hypothesis of independence.

3.4.2 Output

The algorithm outputs Partial Ancestral Graphs (PAGs). PAG are using the following notation:

- **Directed edge** ($X \rightarrow Y$): Possible direct causation from X to Y. In graph theory, X is a parent or ancestor of Y
- **Bidirected edge** ($X \leftrightarrow Y$): Indicates that there is a latent confounder between X and Y. X and Y are neither ancestors nor descendants of each other.
- **Undirected edge** ($X - Y$): Indicates association without orientation. No causal direction is implied. X and Y are both ancestors and descendants of each other.
- **Circle endpoint** ($X \circ\!\!-\!\!\circ Y$, $X \circ\!\!\rightarrow Y$): Represents uncertainty about the direction or presence of latent variables. The circle ($\circ$) denotes ambiguity in orientation.

3.4.3 Algorithm Workflow

1. Skeleton Construction
    - Initialization: Start with a fully connected complete undirected graph that has $\circ\!\!-\!\!\circ$ edge between every pair of variables.
    - Edge Removal: For each pair of variables X and Y:

- Test conditional independence $X \perp\!\!\!\perp Y \mid S$ for conditioning sets $\mathbf{S}$ of increasing size.
- Remove the edge $X - Y$ if a separating set S is found (X and Y are independent given $\mathbf{S}$) and add save the separating set $\mathbf{S}$ as Sepset(X, Y).
- This phase uses a stepwise approach, testing conditioning sets $\mathbf{S}$ of increasing size $k = 0, 1, 2, \ldots$ until no more edges can be removed.

2. Collider Orientation (Unshielded Triples) or $\mathcal{R}0$ (Appendix B)

   - Identify unshielded triples $X - Y - Z$ (where X and Z are not adjacent).
   - Orient $X \rightarrow Y \leftarrow Z$ (a collider) if and only if Y is **not** in the separating set of X and Z.

3. Possible-D-Sep Phase and Edge Orientation

   - Possible-D-Sep Set: For each pair X, Y, compute a superset of variables that could d-separate them in the presence of latent confounders.
   - Additional Conditional Tests: Re-test independence between X and Y conditioned on subsets of their Possible-D-Sep sets.
   - Edge Orientation Rules:
     - Apply orientation rules $\mathcal{R}1-4$(Appendix B) to propagate edge directions. Apply the rules until none of them can be applied.
     - Bidirected edges ($\leftrightarrow$) are added when latent confounding is inferred.

FCI is said to be sound and complete when all assumptions are fulfilled.

3.4.4 Example

1. Input: Observational data on variables X, Y, C, D. Latent confounders and selection bias may be present.

2. Skeleton: CI tests remove edges: $X \perp\!\!\!\perp Y \Rightarrow$ remove $X - Y$ $C \perp\!\!\!\perp D \,|\, Y \Rightarrow$ remove $C - D$

3. Collider Detection: Triple $X - Y - C$: if $Y \notin \text{Sep}(X, C)$, orient as collider:

$$X \rightarrow Y \leftarrow C$$

4. Latent Confounding: $Y \not\perp\!\!\!\perp D$ under all conditions $\Rightarrow$ hidden confounder $\Rightarrow$

$$Y \leftrightarrow D$$

5. PAG Output:

$$X {\circ\!\!\rightarrow} Y {\leftarrow\!\!\circ} C, \quad Y \leftrightarrow D$$

3.5 Advantages and Limitations

Advantages

One key advantage of the FCI algorithm is its ability to handle latent confounding, because FCI does not assume causal sufficiency. This makes it more suitable for real-world data where unmeasured (latent) variables may influence the observed relationships. Additionally, FCI generates a PAG, which offers a more nuanced view of causal structures compared to the CPDAG produced by PC. Furthermore, the equivalence classes are consistent with the observed conditional independencies that may involve latent variables and potential selection bias.

Limitations

A significant limitation of the FCI algorithm is its computational complexity, particularly for datasets with a large number of variables. The CI tests required at each step scale poorly, and exhaustive testing can be computationally intensive. Furthermore, the algorithm is sensitive to errors in CI tests. Inaccuracies in CI testing due to small sample sizes, noise, or incorrect test choice can lead to incorrect edge removals or orientations. These mistakes may propagate through the algorithm and render inaccurate or ambiguous causal inferences in the final PAG.

4 Implementation

All code is available on GitHub DNedilko/CausalDiscovery. The main language of implementation is Python.

4.1 Causal Discovery Setup

Causal Discovery implementation is in the fci_runner.py on GitHub. The workflow of the Python code begins with data preparation. The data_loader function ingests a specified subset of columns from a large dataset (HBSC) and has the option to stratify by sex. This data is then cleaned using the data_prep function, which removes rows with missing values according to the specifications outlined in Data Section and converts the data into a numeric format suitable for subsequent analysis. Textual categorical values are label-encoded, and the DataFrame is transformed into a NumPy array. This ensures that the resulting matrix meets the requirements of the libraries being used.

After data preparation, the pipeline executes the FCI algorithm. The run_fci function applies FCI from `causal-inference` package to the cleaned data, utilising G^2 and χ^2 as the conditional independence test at a specified significance level. The output is a Partial Ancestral Graph (PAG) that encodes the inferred causal relationships among variables. This graph is then visualised and saved as a PNG image. To facilitate a comprehensive analysis, the `iterator_over_fci` function performs parallel execution of FCI across multiple conditional independence tests and significance levels.

The used `causal-learn` library follows the algorithm in the Methodology. Besides that, it allows for background knowledge. This function enables the restriction of testing sets during the adjacency identification step of FCI[1]. Example of use is available in the Appendix C.

4.2 Parameter Choices

The conditional independence (CI) tests G^2 and χ^2 are asymptotically similar. To assess which test would perform better in terms of runtime, we experimented by comparing their scalability. We found that, for the given dataset, the χ^2 test scaled less efficiently. This may be since the G^2 test handles zero counts more robustly and relies on logarithmic operations (see Figure 2).

Furthermore, G^2 is more stable under changes in the significance level α, and its runtime does not increase as sharply compared to the χ^2 test(see Figure 3). Based on these findings, we chose the G^2 test for all subsequent experiments.

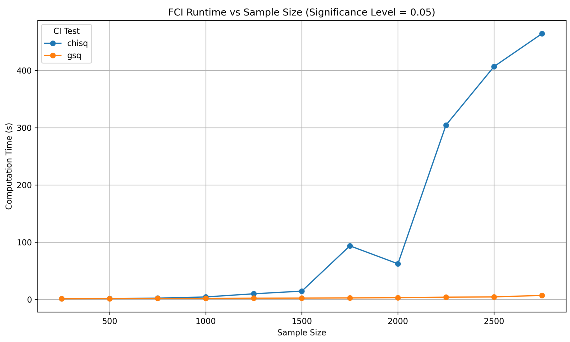

Figure 2: Computation time of the FCI algorithm as a function of sample size for different CI tests. The significance level α is fixed at 0.05 to isolate the effect of increasing data volume on performance.

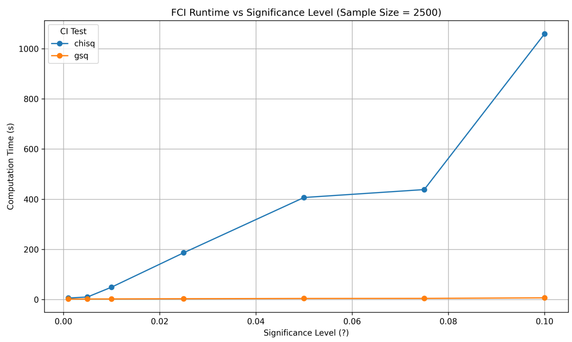

Figure 3: Computation time of the FCI algorithm across different significance levels α for various conditional independence (CI) tests. Results are based on a fixed sample size of 2500 observations.

During the experiments, we ran through $\alpha = [0.001, 0.01, 0.05, 0.1]$. We also test how differently χ^2 and G^2 will perform given $\alpha = 0.01$ on 6660 samples.

5 Analysis of Results

5.1 Learned Causal Structure

Figures 6 to 13 depict the PAGs obtained using the FCI algorithm under various parameter configurations. For the subset comprising 27 variables, lower significance levels (e.g., $\alpha = 0.001$) yielded relatively sparse graphs, whereas higher levels (e.g., $\alpha = 0.05$) resulted in denser structures. For interpretative analysis, we focus on the graph presented in Figure 8, as it appears to offer a plausible and coherent representation of real-world relationships while also maintaining greater clarity and interpretability compared to the more complex graphs produced from the 78-variable subset (Figures 11 to 13, see Appendix D).

5.2 Interpretation

The selected graph in Figure 8 exhibits a modular structure, with variables organised into four thematically coherent clusters.

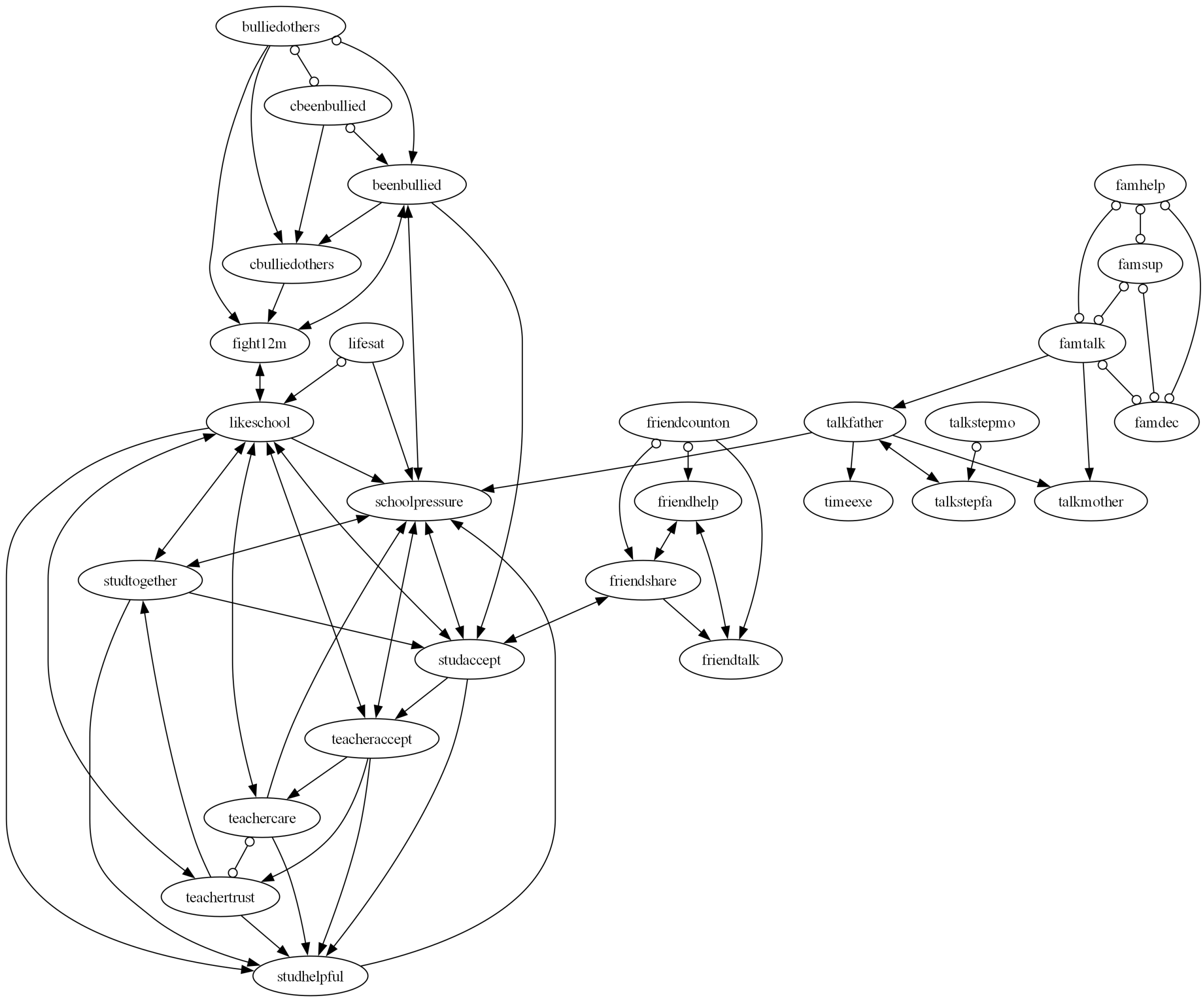

Figure 4: Findings from the FCI algorithm with G^2, performed at a significance level of 0.05.

Bullying cluster

beenbullied emerges as the central node within the bullying cluster and aligns with meta-analytic findings indicating that bullying victimisation functions both as a consequence of prior aggressive behaviours and as a catalyst for a wide range of adverse outcomes[5], the node directed edges from cbeenbullied and bulliedothers, with bidirected edges indicating potential latent confounding. It acts as a probable direct cause of cbulliedothers and fight12m, the latter also exhibiting a bidirected edge suggestive of an unmeasured common cause. Additionally, studaccept appears to be directly influenced by beenbullied. It might be explained by the fact that bullying victims feel unwelcome in social settings, as it adds pressure to peer-to-peer communication between students. Oftentimes, students avoid others who are being bullied for fear that they might be the next victim of bullying. A latent confounder is implied between schoolpressure and beenbullied. It could be a rival at school or a setting at school.

bulliedothers is directly linked to both cbulliedothers and fight12m, indicating that adolescents who bully others are likely to engage in both cyberbullying and physical aggression. Although the causal direction between cbeenbullied, cbulliedothers, and beenbullied is partially unresolved, the connectivity suggests a strong interplay between online and offline bullying experiences. These relations are supported by modern research. Longitudinal studies demonstrate bidirectional relationships between traditional and cyberbullying behaviours, with approximately 56% of online bullies also engaging in face-to-face bullying[2].

cbulliedothers further influences fight12m, highlighting a potential pathway from cyberbullying perpetration to physical violence. In turn, fight12m affects likeschool, suggesting that involvement in violent behaviours negatively impacts students' school engagement[5].

School environment and friendship clusters

The school environment and friendship clusters are interconnected, mirroring real-life situations where academic, peer, and friendship contexts overlap. At the centre of the school environment cluster is studhelpful, which is directly influenced by teachertrust, teacheraccept, teachercare, and studtogether. This suggests that helpfulness in a learning context emerges from relational dynamics with both teachers and peers. An understanding and accepting teacher might propagate their attitude to students. An edge from likeschool to studhelpful would also make sense in the opposite direction, as we would expect that students being helpful toward an individual could influence that individual's liking of school.

teachertrust, in particular, exhibits strong connectivity and may serve as a proxy for a safe and supportive school climate. Its bidirected edges to teachercare and teacheraccept suggest potential unmeasured common causes. These variables also feed into studaccept; together with schoolpressure, they appear to have a latent confounder. likeschool likely has a direct influence on schoolpressure. This suggests that students who feel accepted and enjoy school are less likely to experience it as a source of pressure.

The friendship cluster emerges around friendhelp, friendtalk, and friendcounton, with bidirected edges between them suggestive of latent variables, possibly suggesting general trust as a latent confounder. These nodes are tightly linked to friendshare and, through a bidirected edge, to studaccept, which acts as a bridge into the academic cluster. This connection may suggest that, given a certain latent confounder, such as whether friends are schoolmates or not, positive and accepting friendships can foster peer acceptance within the school.

Parental and family communication cluster

As expected, the family cluster is dense and tightly linked to parental support. The graph, however, represents uncertainty in causal directions within the family segment. Several connections involve edges with open circles, likely reflecting the complexity of family structures and latent variables, which may indicate a particular communication style or external, unaccounted forces that influence the family.

famsup appears to be the centre of the family support cluster. In real life, the feeling of being supported arises from the ability to communicate, solve problems together, and assist one another in times of need. famtalk serves as a bridge between the general family context and specific parental communication variables. Communication quality within a family likely acts as a direct cause of high-quality individual communication between parents and children.

Interestingly, timeexe has a direct edge to talkfather, implying that a positive relationship with one's father may encourage more physical activity or shared activities. The parental communication cluster also includes a direct edge from talkfather to schoolpressure, suggesting that good communication with one's father may reduce feelings of academic pressure, which could possibly be mediated by latent variables such as self-confidence or a sense of being supported at home.

General takeaway

The bullying cluster, in particular, is notably intertwined with both academic and social spheres. These links back up the idea that bullying is not an isolated experience but rather a social phenomenon that occurs across both online and offline settings. The presence of bidirected edges in the cluster (between beenbullied and schoolpressure) suggests that latent variables may underlie multiple observed associations. This may point to broader constructs such as general emotional vulnerability, peer reputation, or school climate as potential shared causes.

5.3 Comparison of 27-variable and 78-variable Graphs

To examine the stability of the learned causal structure, we compared two PAGs produced by the FCI algorithm using subsets of the HBSC dataset: one with 27 variables (Figure 8) and another with 78 variables (Figure 13). We aimed to assess whether the smaller graph captures core causal patterns and to what extent it can be viewed as a projection of the more complex structure.

The comparison shows a notable degree of overlap. Both graphs contain the main clusters: bullying, school engagement, peer relationships, and family communication. They share key variables such as beenbullied, cbulliedothers, schoolpressure, studaccept, and famtalk. Many directional edges are consistent across graphs. For instance, cbulliedothers → fight12m is preserved (with bulliedothers added as a mediator in the larger graph), as are teachertrust → studhelpful and schoolpressure → studaccept.

A notable difference is the reduced role of the friendship cluster. In the 27-variable graph, nodes like friendhelp, friendtalk, and friendcounton are tightly connected and influence school-related outcomes. In the larger graph, these nodes are present but more isolated and with undefined relations within, suggesting that peer communication becomes less central when emotional and contextual variables are taken into account.

The 78-variable graph introduces additional complexity. It includes psychosomatic symptoms (`headache`, `sleepdifficulty`), emotional indicators (`emosome01`–`emosome08`), and detailed family and socioeconomic variables (e.g., `fatherhome1`, `employfather`, `fascomputers`). These increase graph density and add new mediating paths. For example, while `lifesat` is mainly influenced by school and peers in the smaller graph, it connects to emotional and health variables in the larger one, pointing out to missing mediators in the reduced version.

Some relationships also change. In the 27-variable graph, `talkfather` directly influences `schoolpressure`. This link remains in the 78-variable graph but is now embedded within a bigger neighbourhood, including `employfather`, which may confound or mediate the relationship.

Although all 27 variables are present in the larger model, the smaller graph is not a strict subgraph. While many patterns are preserved, new edges and latent confounding structures emerge.

5.4 Sensitivity to Parameters

Variables	CI test	α	Time (s)	Resulting graph
27	G^2	0.001	18	6
27	χ^2	0.001	4516	10
27	G^2	0.010	23	7
27	G^2	0.050	446	8
78	G^2	0.001	263	11
78	G^2	0.010	5851	12
78	G^2	0.050	19390	13

Table 3: Summary of optimal parameters search for FCI algorithm with corresponding time required for execution. The experiments were run on 6660 records with different subsets of variables.

5.4.1 Effect of Increasing α

To investigate the sensitivity of the learned PAG structure to changes in the CI threshold, we compared graphs generated with the FCI algorithm using α levels of 0.001, 0.01, 0.05, and 0.1(Figures 6 to 9). As α increases, the CI tests become more permissive, as more edges appear in the graph.

At $\alpha = 0.001$, the PAG is sparse and includes only the strongest dependencies. Many nodes appear isolated or weakly connected, especially those in the friendship or well-being domains. As α increases, the number of edges grows noticeably. At $\alpha = 0.05$, core clusters become more densely connected, and by $\alpha = 0.1$, the graph becomes highly saturated.

Across all values of α, `schoolpressure` remains a highly connected node. As the threshold increases, it forms connections to variables such as `beenbullied`, `lifesat`, and `talkfather`, which bridge between academic stress, social dynamics, and family communication.

The number of bidirected edges, or identified latent confounding patterns, increases with α. Notably, these appear among variables such as `teachertrust` and `teachercare`, or `beenbullied` and `schoolpressure`.

At lower α values, the family communication variables are mostly self-contained and have no causal directions. As α increases, variables like `talkfather` begin to connect with school-related outcomes, including `schoolpressure` and `lifesat`.

Increasing α in the FCI algorithm results in denser graphs with more discovered edges and a higher prevalence of latent confounding structures. The graph at $\alpha = 0.05$ appears to show a balance between interpretability and coverage relations within data. It maintains the clustering while capturing meaningful dependencies. Lower α values yield cleaner, more conservative graphs suitable for high-confidence interpretations, while higher α values expose richer and more exploratory causal pathways. However, despite the benefits of causal graphs, they should be carefully reviewed and interpreted in conjunction with background knowledge and alternative research.

5.4.2 CI test role

To isolate the effect of the CI test used, we compared two PAGs estimated at the same significance level $\alpha = 0.001$: one using the G^2 test (Figure 6) and the other using the χ^2 test (Figure 10).

The graph based on the χ^2 test is significantly denser than the one based on G^2, with more directed and bidirected edges across clusters, higher connectivity, and more inferred causal and confounding relationships.

In the χ^2 graph, the friendship cluster (`friendhelp`, `friendcounton`, `friendshare`, `friendtalk`) is tightly connected and links to broader constructs such as `lifesat`, `famsup`, and `schoolpressure`. The family communication variables are also more integrated, while they form edges with both school-related and emotional variables. In contrast, the G^2 graph presents these clusters as disconnected, with `lifesat` entirely disconnected and minimal influence from peer or family support pathways.

Both graphs preserve the core components of the school and bullying clusters. However, the G^2 graph shows a more detailed picture: for example, `beenbullied` connects to both `schoolpressure` and `lifesat`. Additionally, the χ^2 graph includes bidirected edges between `cbulliedothers` and `cbeenbullied`, as well as between schoolpressure and friendshare, indicating latent confounding. Such patterns are mainly absent in the G^2 graph, where the bullying variables remain internally clustered with undefined paths but disconnected from other domains.

6 Discussion

This study used the Fast Causal Inference (FCI) algorithm to explore causal relationships in adolescent bullying behaviour based on the 2018 HBSC dataset. The output is a Partial Ancestral Graph (PAG), a representation that encodes causal and ancestral relations under the assumption of potential latent confounding and selection bias. As such, the output does not fully orient all edges but provides a consistent representation of the underlying equivalence class of causal structures. This enables us to interpret the results carefully, suggesting strong dependencies yet not always clear cause-and-effect directionality.

Across multiple settings, *beenbullied* consistently appeared as a central node, connected to *cbulliedothers*, *fight12m*, and *studaccept*. These findings imply a connection between victimisation, aggressive conduct, and social integration. Interestingly, direct measures of digital device usage did not serve as significant causes, which contrasts with prevalent assumptions regarding smartphones' direct influence on cyberbullying. Instead, the results endorse the perspective that wider psychosocial factors, such as peer relationships and academic experiences, influence bullying behaviours.

The causal structure varied significantly with the choice of the conditional independence (CI) test and the significance level α. Graphs generated using the G^2 test were generally sparser and more interpretable than those from χ^2, which tended to produce denser structures. Lower α thresholds (e.g., 0.001) yielded conservative graphs, reducing potential false positives, while higher thresholds increased edge count at the cost of interpretability. An α level of 0.01 with the G^2 test was found to offer a good trade-off between complexity and robustness.

The assumptions behind FCI, particularly the Causal Markov Condition and Faithfulness, are essential for valid inference. Although these assumptions are standard in causal discovery, their applicability to social survey data is not guaranteed. Furthermore, because of the observational and cross-sectional characteristics of the HBSC data, along with the discretisation necessary for the algorithm, causal claims ought to be understood in a structural context. The outcome causal paths should be carefully reviewed and interpreted in conjunction with background knowledge and broader behavioural analysis knowledge.

Bidirected edges in the PAG indicate the presence of latent confounding. These likely correspond to unmeasured psychological traits, familial factors, or environmental variables not included in the HBSC survey. Their existence emphasises the strength of FCI in handling partially observed systems and highlights the need for further data collection in future studies.

In general, the inferred relationships are structurally sound and largely align with current psychological and sociological research. Importantly, the limited causal influence of technology-related factors challenges prevailing assumptions held by the general public and points to avenues for future research.

7 Conclusion

This study applied the FCI algorithm to explore the causal structure underlying bullying and cyberbullying among Ukrainian adolescents using cross-sectional data from the 2018 HBSC survey. By leveraging conditional independence tests and accounting for potential latent confounding, we produced Partial Ancestral Graphs that revealed consistent patterns of interaction among behavioural, social, and academic factors.

The results emphasise the centrality of peer victimisation within a network of aggression, academic stress, and social acceptance. Contrary to common expectations, digital device usage did not emerge as a dominant causal factor, suggesting that cyberbullying reflects existing offline dynamics rather than being driven primarily by technology. This finding underscores the importance of addressing underlying social and emotional determinants rather than focusing solely on digital access or media exposure.

Methodologically, the analysis demonstrates the sensitivity of constraint-based causal discovery to choices of test statistic and significance threshold. An α level of 0.01 combined with the G^2 test yielded the most interpretable and stable structures, balancing false discovery control with model complexity.

While the observational and self-reported aspects of the dataset restrict the ability to make strong causal claims, the structural insights gathered are significant and typically consistent with theoretical expectations. Nevertheless, these results should be interpreted cautiously and verified by field experts. Future research could enhance this analysis by integrating longitudinal data, various psychosocial variables, and different causal discovery techniques to validate and fine-tune the inferred relationships.

References

[1] *causal-learn: Causal discovery in Python*. https://causal-learn.readthedocs.io/en/latest/. Accessed: 2025-06-13. 2025.

[2] Anke Görzig and Hana Machackova. "Cyberbullying from a socio-ecological perspective: A contemporary synthesis of findings". In: *Psychology of Violence* 5.3 (2015), pp. 231–244. DOI: 10.1037/a0034564.

[3] HBSC Data Management Centre, University of Bergen. *HBSC-2017/18, Overview (Version 1.0)*. https://www.uib.no/sites/w3.uib.no/files/attachments/hbsc2018oaed1.0.pdf. Data file and documentation accessed: 10 June 2025; Dataset contains public open-access variables list and overview. 2018.

[4] Neville Kenneth Kitson et al. "A survey of Bayesian Network structure learning". In: *Artificial Intelligence Review* 56.8 (2023), pp. 8721–8814. DOI: 10.1007/s10462-022-10351-w. URL: https://doi.org/10.1007/s10462-022-10351-w.

[5] Chao Li et al. "Traditional bullying and cyberbullying in the digital age and its associated mental health problems in children and adolescents: a meta-analysis". In: *European Child & Adolescent Psychiatry* 33.9 (Sept. 2024). Epub 2022 Dec 31, pp. 2895–2909. DOI: 10.1007/s00787-022-02128-x. URL: https://doi.org/10.1007/s00787-022-02128-x.

[6] Jiji Zhang. "On the completeness of orientation rules for causal discovery in the presence of latent confounders and selection bias". In: *Artificial Intelligence* 172.16 (2008), pp. 1873–1896. ISSN: 0004-3702. DOI: 10.1016/j.artint.2008.08.001. URL: https://www.sciencedirect.com/science/article/pii/S0004370208001008.

[7] Chengyan Zhu et al. "Cyberbullying Among Adolescents and Children: A Comprehensive Review of the Global Situation, Risk Factors, and Preventive Measures". In: *Frontiers in Public Health* 9 (2021), p. 634909. DOI: 10.3389/fpubh.2021.634909. URL: https://www.frontiersin.org/articles/10.3389/fpubh.2021.634909/full.

A Correspondance of FASIII and Relative FASIII scores

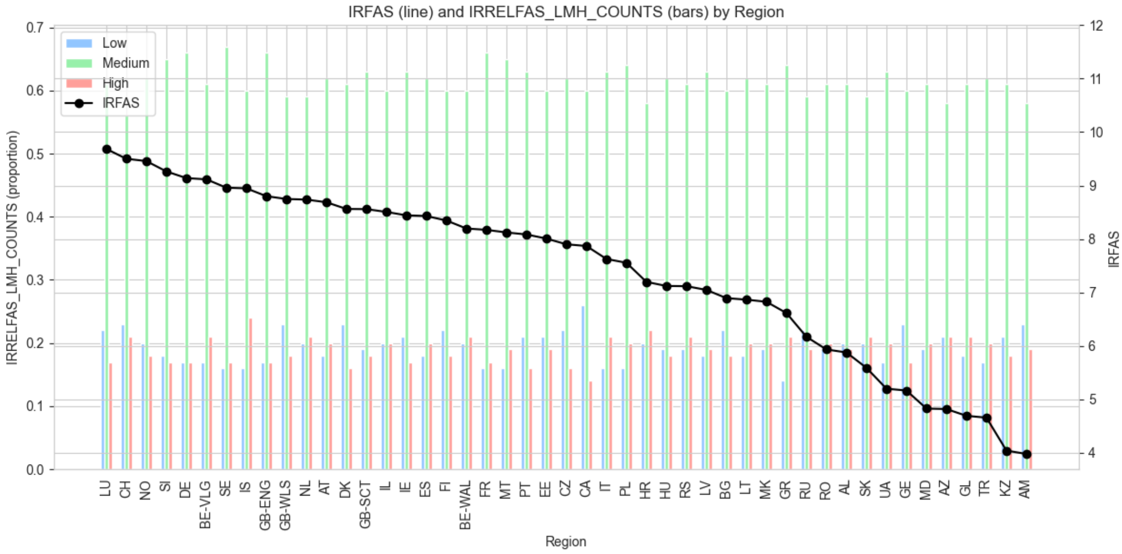

Figure 5: Comparison of weighted average Family Affluence Score (IRFAS, black line) and the distribution of relative family affluence categories (Low, Medium, High; colored bars) across regions. Regions are ordered by descending IRFAS. The left y-axis shows the proportion of each affluence category, while the right y-axis displays the average IRFAS

B Meek's Rules for FCI

$\mathcal{R}0$. (Unshielded Collider)
If $X *\!-\!* Y *\!-\!* Z$, and X and Z are not adjacent, and $Y \notin \mathrm{SepSet}(X, Z)$,
then orient as $X *\!-\!> Y <\!-\!* Z$.

$\mathcal{R}1$: If $X *\!-\!* Y \circ\!-\!* Z$, and X and Z are not adjacent, then orient as $X *\!-\!* Y \to Z$.

$\mathcal{R}2$: If $X \to Y *\!-\!* Z$ or $X *\!-\!* Y \to Z$, and $X *\!-\!\circ Z$,
then orient $X *\!-\!\circ Z$ as $X *\!-\!* Z$.

$\mathcal{R}3$: If $X *\!-\!* Y \leftrightarrow Z$, $X *\!-\!\circ M \circ\!-\!* Z$, X and Z are not adjacent, and $M *\!-\!\circ Y$,
then orient $M *\!-\!\circ Y$ as $M *\!-\!* Y$.

$\mathcal{R}4$: If $u = (M, \ldots, X, Y, Z)$ is a discriminating path between M and Z for Y,
and $Y \circ\!-\!* Z$; then if $Y \in \mathrm{SepSet}(M, Z)$, orient $Y \circ\!-\!* Z$ as $Y \to Z$;
otherwise orient the triple (X, Y, Z) as $X \leftrightarrow Y \leftrightarrow Z$.

$\mathcal{R}5$: For every (remaining) $X \circ\!-\!\circ Z$, if there is an uncovered circle path $p = (X, M, \ldots, K, Z)$
between X and Z such that X, K are not adjacent and Z, M are not adjacent,
then orient $X \circ\!-\!\circ Z$ and every edge on p as undirected edges $(-)$.

$\mathcal{R}6$: If $X *\!-\!* Y \circ\!-\!* Z$ (X and Z may or may not be adjacent),
then orient $Y \circ\!-\!* Z$ as $Y \to Z$.

$\mathcal{R}7$: If $X \circ\!-\!\circ Y \circ\!-\!* Z$, and X, Z are not adjacent, then orient $Y \circ\!-\!* Z$ as $Y \to Z$.

$\mathcal{R}8$: If $X \to Y \to Z$ or $X \circ\!-\!\circ Y \to Z$, and $X \circ\!-\!Z$, orient $X \circ\!-\!Z$ as $X \to Z$.

$\mathcal{R}9$: If $X \circ\!-\!Z$, and $p = (X, Y, M, \ldots, Z)$ is an uncovered p.d. path from X to Z
such that Z and Y are not adjacent, then orient $X \circ\!-\!Z$ as $X \to Z$.

$\mathcal{R}10$: Suppose $X \circ\!-\!Z$, $Y \to Z \leftarrow K$, p_1 is an uncovered p.d. path from X to Y,
and p_2 is an uncovered p.d. path from X to K.
Let M be the vertex adjacent to X
on p_1 (M could be Y), and A be the vertex adjacent to X on p_2 (A could be K).
If M and A are distinct, and are not adjacent, then orient $X \circ\!-\!Z$ as $X \to Z$.

Here, all nodes $X, Y, Z, M, K, A \in \mathbf{V}$, the set of nodes in the graph.
$\mathcal{R}0$-$\mathcal{R}3$ are the inference rules for learning DAGs. $\mathcal{R}4$ is specific to MAGs with bidirected edges. $\mathcal{R}5$-$\mathcal{R}6$ are irrelevant if the true causal MAG does not contain undirected edges (e.g., no selection bias). $\mathcal{R}7$ might not be triggered because none of $\mathcal{R}0$-$\mathcal{R}4$ and $\mathcal{R}8$-$\mathcal{R}10$ lead to $-\!\circ$. $\mathcal{R}8$-$\mathcal{R}10$ help convert partially directed edges into directed ones, and together they render an Augmented FCI[6].

C Python causal-learn FCI example

```
import numpy as np
import pandas as pd
from causallearn.search.ConstraintBased.FCI import fci
from causallearn.utils.cit import gsq
from causallearn.utils.GraphUtils import GraphUtils


def run_fci(
    data: pd.DataFrame,
    test: = "gsq",
    alpha: float = 0.05) -> tuple:

    data_array = data.values.astype(np.float32)

    # Run FCI with specified parameters
    graph, edges = fci(
        dataset=data_array,
        independence_test_method=test,
        alpha=alpha,
        verbose=True
    )

    # Generate agraph visualisationn
    GraphUtils.to_pydot(graph, labels=data.columns.tolist())
            .write_png(
                os.path.join(output_dir, filename)                    )
    return graph, edges

    run_fci(data, test = gsq, alpha = 0.05)
```

D Graphs for 27 and 78 variables at significance levels 0.01, 0.001 and 0.05

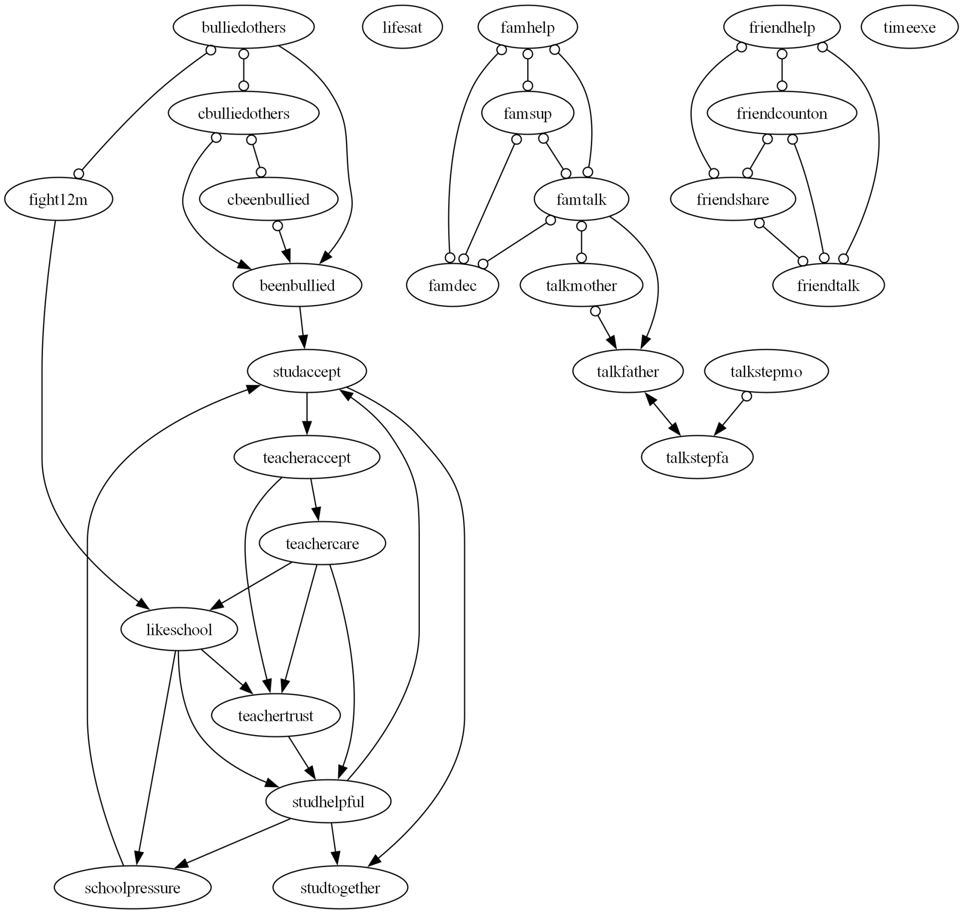

Figure 6: Findings from the FCI algorithm with G^2, performed at a significance level of 0.001.

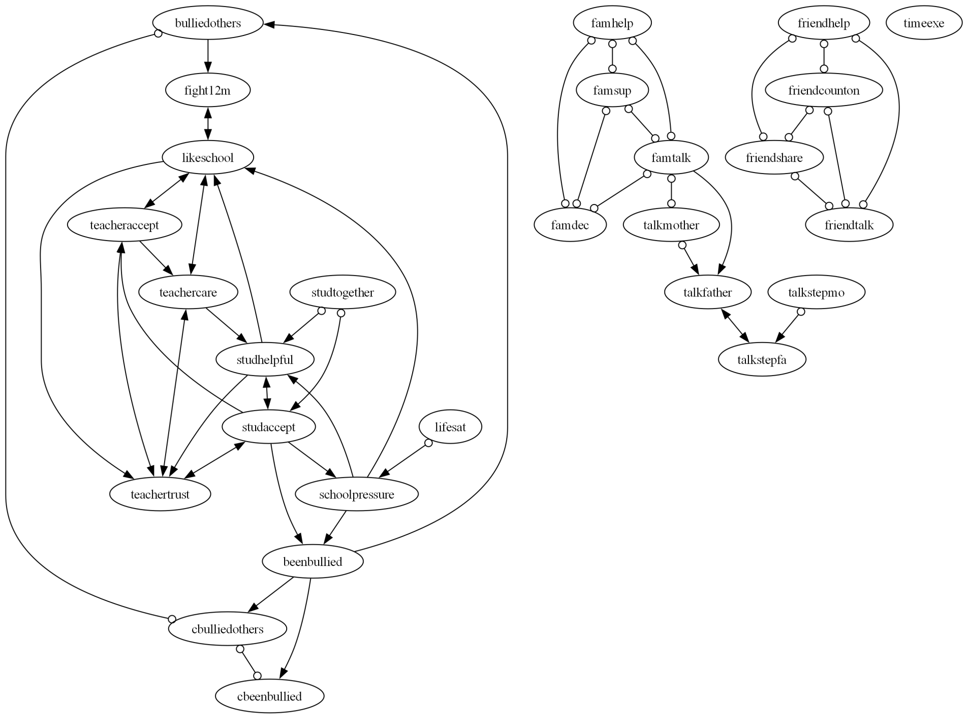

Figure 7: Findings from the FCI algorithm with G^2, performed at a significance level of 0.01.

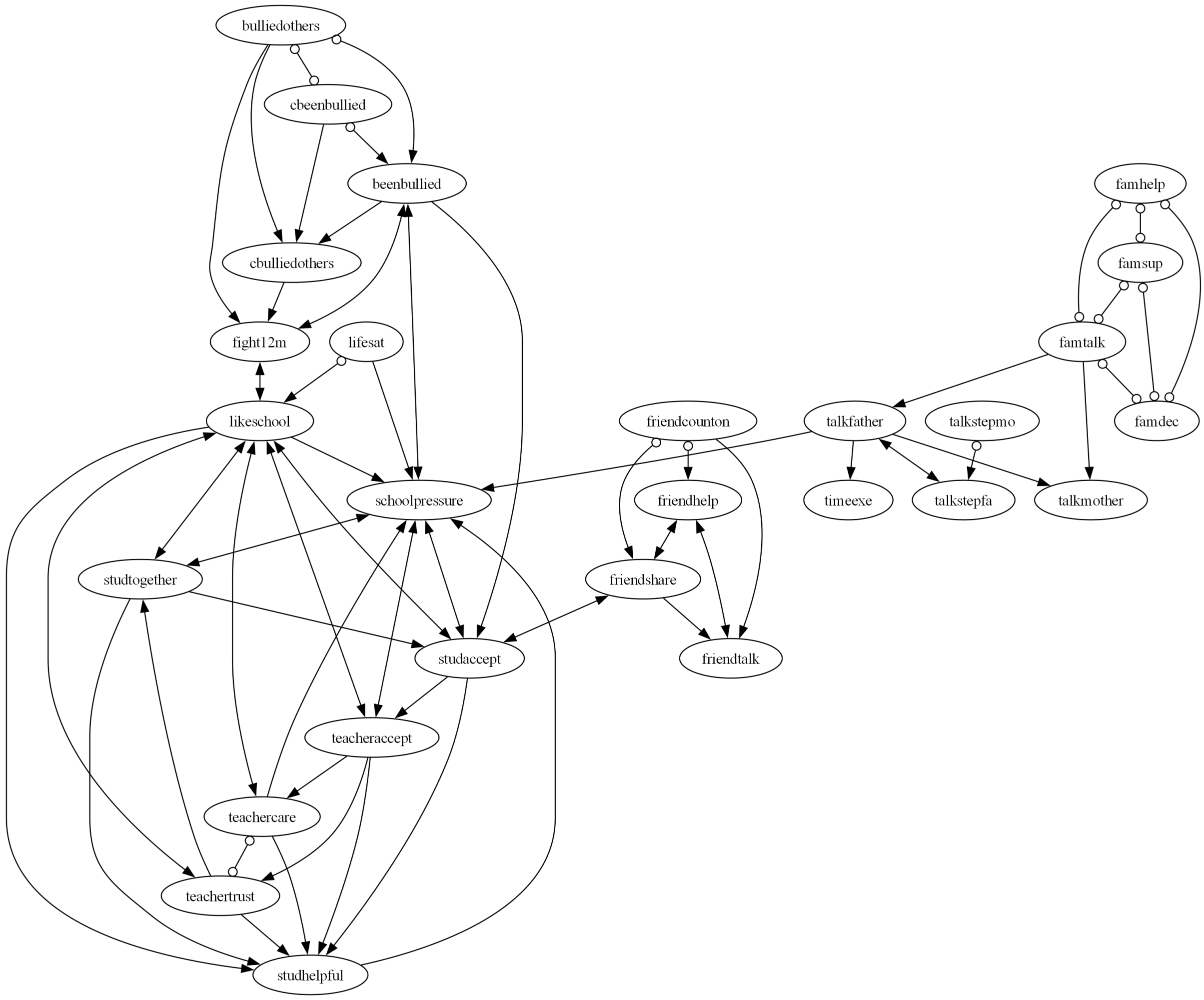

Figure 8: Findings from the FCI algorithm with G^2, performed at a significance level of 0.05.

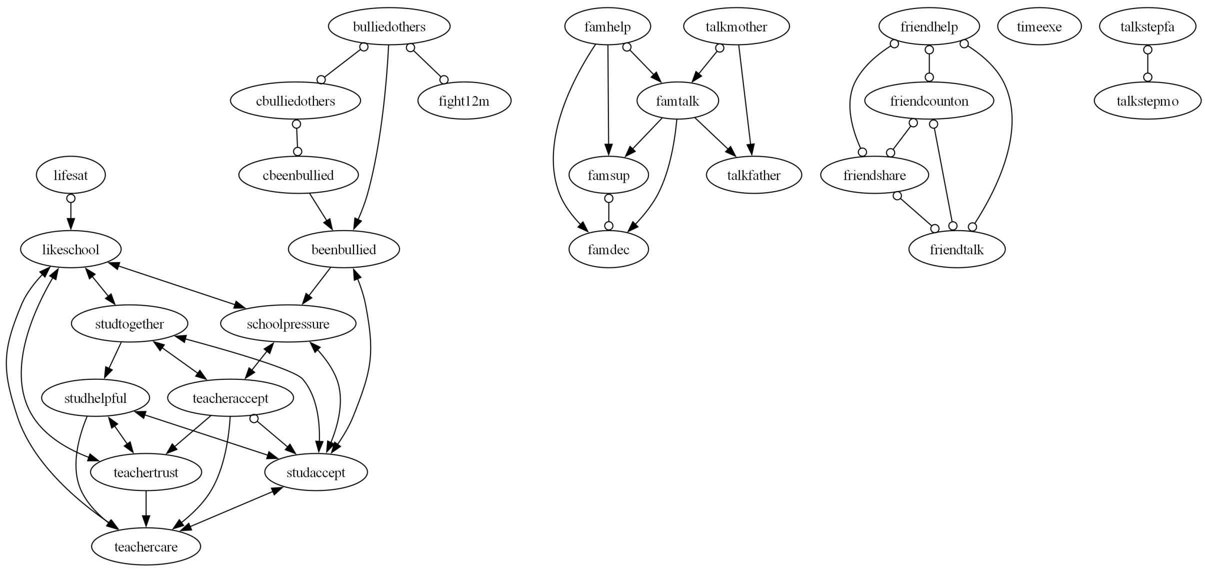

Figure 9: Findings from the FCI algorithm with gsq, performed at a significance level of 0.1

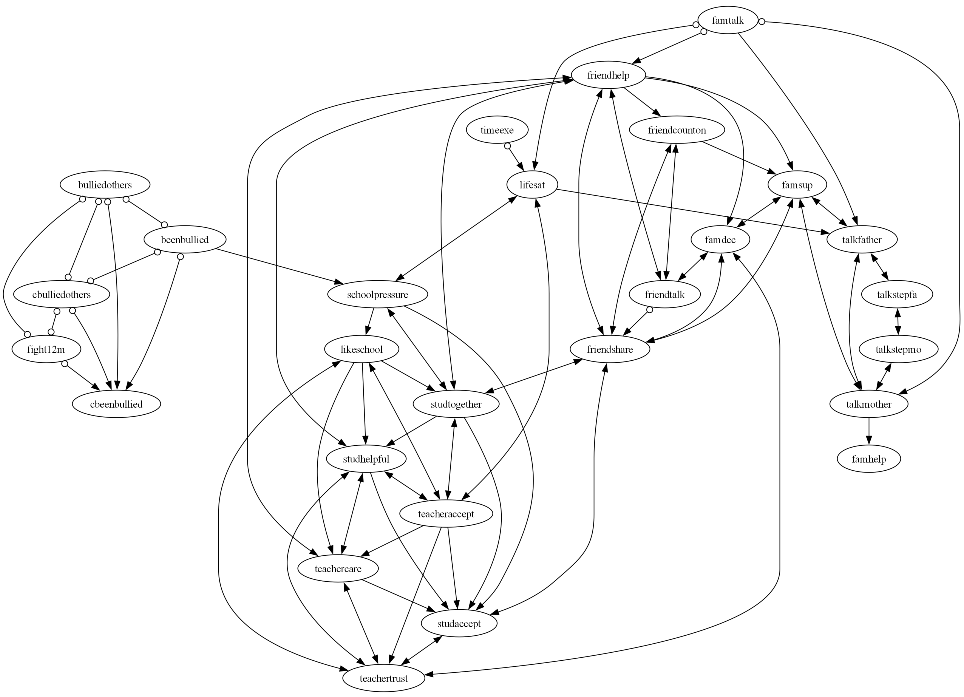

Figure 10: Findings from the FCI algorithm with χ^2, performed at a significance level of 0.001.

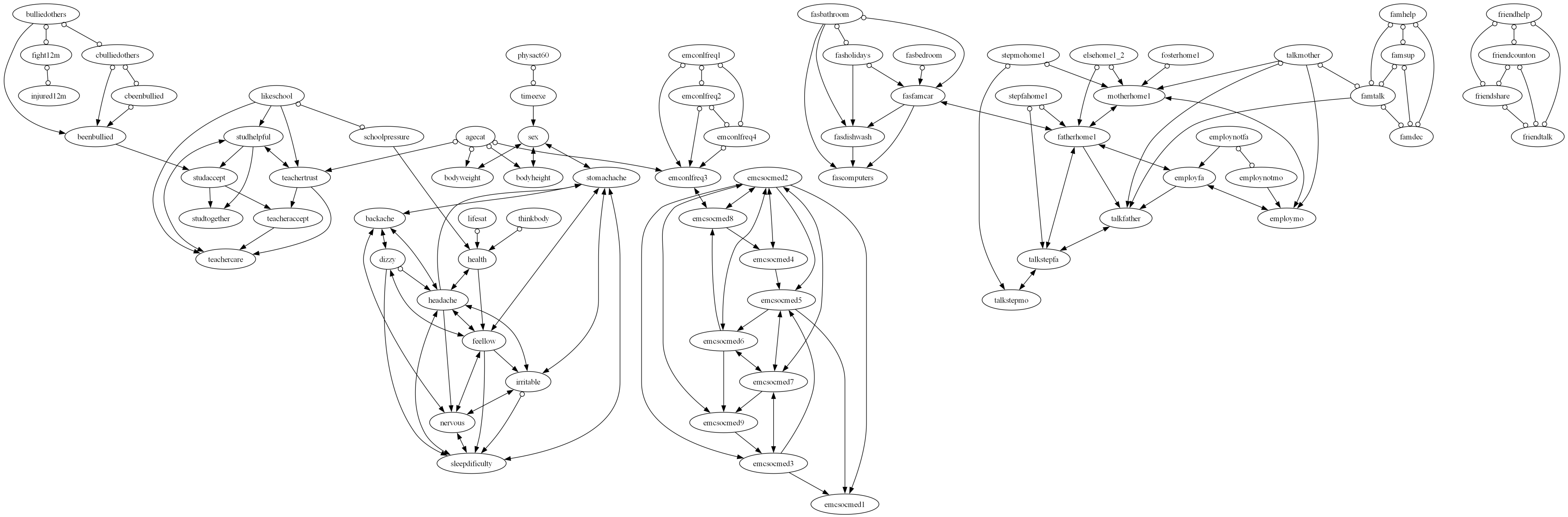

Figure 11: Findings from the FCI algorithm with G^2, performed at a significance level of 0.001

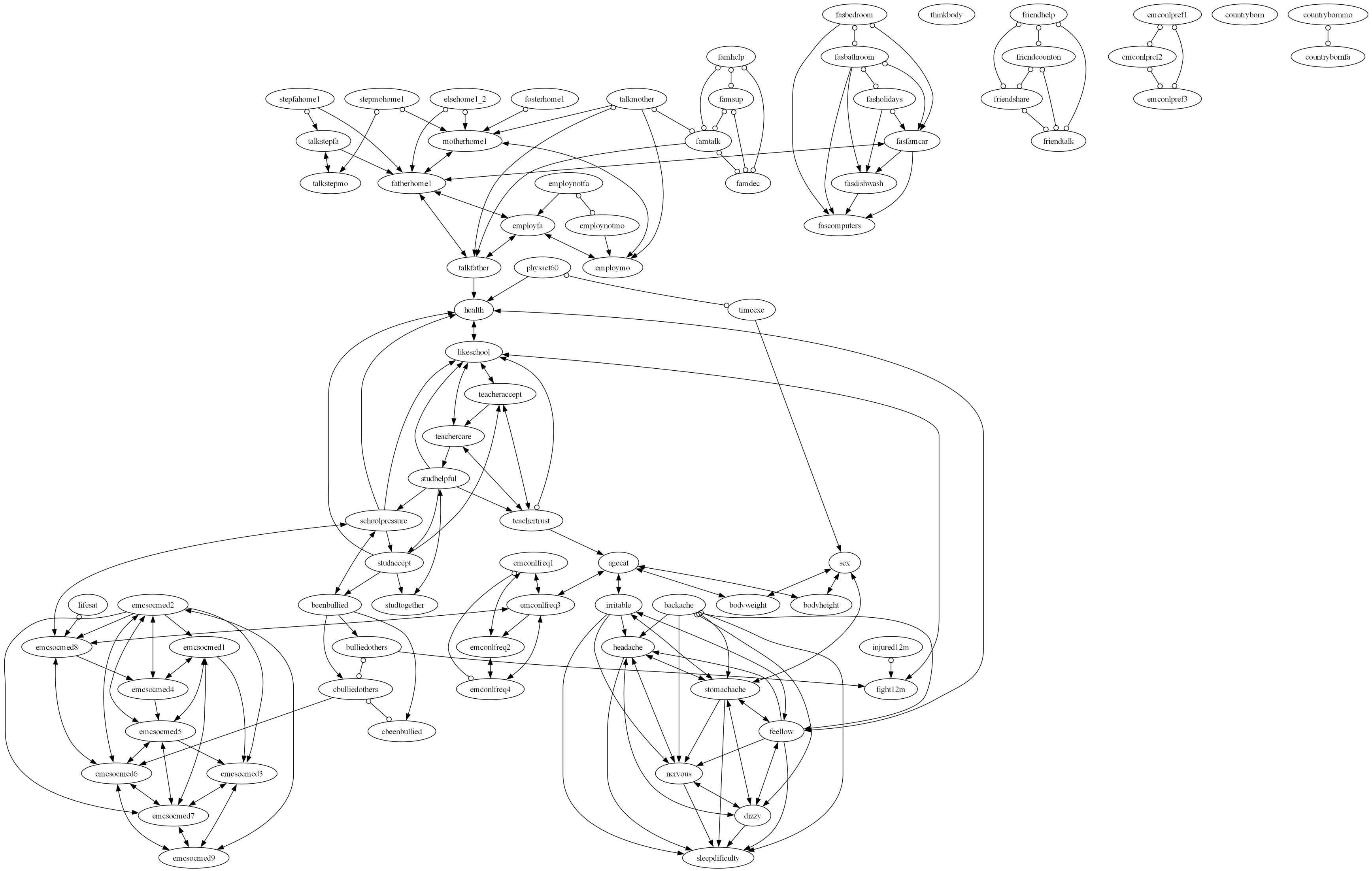

Figure 12: Findings from the FCI algorithm with G^2, performed at a significance level of 0.01

Figure 13: Findings from the FCI algorithm with G^2, performed at a significance level of 0.05.